Vol. 40, No. 2 (2018) 274-282, DOI: 10.24874/ti.2018.40.02.11

Tribology in Industry

www.tribology.rs

RESEARCH

A Friction, Wear and Emission Tribometer Study of Non-Asbestos Organic Pins Sliding Against AlSiC MMC Discs

Y. Lyu[a], J. Wahlström[a], M. Tu[a], U. Olofsson[a]

[a]*Department of Machine Design, KTH Royal Institute of Technology, Stockholm, Sweden.*

Keywords:

Disc brake
Wear
Friction
Emission
AlSiC MMC

Corresponding author:

Yezhe Lyu
Department of Machine Design,
KTH Royal Institute of Technology,
Stockholm, Sweden.
E-mail: yezhe@kth.se

A B S T R A C T

The friction, wear and particle emission from an AlSiC MMC brake disc/non-asbestos organic brake pad system is studied using a pin-on-disc tribometer. The results show that this unconventional AlSiC MMC brake disc system presents friction performance as good as a conventional cast iron brake disc system. During braking, brake pad materials are transferred to the brake disc surface to form a protective third body tribo-layer, resulting in a negative specific wear rate of the brake disc. A higher contact load is likely to make it easier to generate the tribo-layer. The tribo-layer also seems to depend on the disc surface grinding features and the contact temperature during braking. By reusing an AlSiC MMC disc where the tribo-layer is already formed, the airborne emission in terms of mass is about 50% lower and in terms of number about the same as the conventional brake contact pair under a similar braking condition. Further full-scale studies are suggested to determine the validity of the findings.

1. INTRODUCTION

Disc brake systems are widely used on cars and trucks for deceleration or braking. A typical disc brake system contains a calliper with several pistons, a rotor and two pads. During braking, the kinetic energy of a vehicle is dissipated by frictional heat between the rotor and the pads. Grey cast iron has been the most commonly used rotor material for decades due to its high thermal conductivity, low cost and easy casting. Since the brake rotor accounts for a considerable part of the chassis weight, a demand for lightweight materials to substitute for cast iron brake rotors is emerging in order to improve fuel efficiency [1]. Aluminium metal matrix composites (MMCs) are thought to be promising materials for brake rotors. MMCs possess some advantages over cast iron, including higher thermal conductivity, lower density, and higher specific strength [2]–[6].

During the braking process, airborne particles are generated by the disc brake system, contributing up to 50 % of the total non-exhaust particle emissions from road transport in the EU [7],[8]. These micro- and nano-size airborne particles have been found to have adverse

effects such as weakening pulmonary antimicrobial immune defence [9], inducing heritable mutations [10], and affecting lung function [11]. Although there are already some standards that limit exhaust emissions, there is no corresponding standard for non-exhaust emissions [12]. Relevant knowledge on the airborne particle emissions from Al MMC brake discs is very scarce.

Currently, most studies of the tribological behaviour of Al MMCs are conducted in laboratories. A number of pin-on-disc tribometer tests have been conducted to investigate the friction and wear performance of Al MMCs with non-asbestos organic (NAO) brake pad materials as the counterpart under varied nominal contact pressures and sliding speeds [13]–[16].

The tribological behaviour of Al MMC brake discs also largely depends on the type [17], number [18], size [19] and shape [14] of the reinforcing particles. Temperature has also been found to strongly affect the friction and wear behaviour of Al MMC brake discs [13],[19],[20], as it may generate a protective tribofilm on the disc surface [3]–[5],[21]–[23].

The present study is intended to investigate the friction, wear and airborne particle emissions from a commercial NAO pad/Al MMC disc contact pair used on C-segment cars in Europe. The main purposes are to determine the effects of normal load on the friction, wear and airborne particle emissions and the tribochemical changes of the Al MMC worn surfaces.

2. EXPERIMENTAL SETUP

2.1 Test equipment

The tests were performed in the same pin-on-disc tribometer test setup described in [23]. In this setup, the disc specimen is mounted horizontally and is rotated by a motor at rotational speeds from 1 to 3000 rpm. The pin specimen is fixed in a stationary pin holder. Dead weights are used to apply different normal loads from 1 to 100 N on the pin specimen, which results in different nominal contact pressures depending on the nominal contact area. The tangential force is measured using an HBM® Z6FC3/20 kg load cell, and the coefficient of friction is determined by dividing this measurement by the applied normal load. The disc temperature is measured with a K-type thermocouple 3 mm below the contact surface.

The mass loss of the test specimens is measured by weighing the test samples before and after the test to the nearest 0.1 mg using a Sartorius® ME614S balance. The specific wear rate for each specimen can then be determined as [24]:

$$k = \frac{\Delta m}{\rho \cdot \Delta s \cdot F_N} \quad (1)$$

where Δm is the mass loss of the specimen, ρ is the density of the specimen, Δs is the sliding distance during the test, and F_N is the normal load applied to the pin. This method enables calculation of the specific wear rate of both pin and disc, but it will include the mass losses from running-in.

The tribometer is placed inside a closed box to enable airborne particle measurements. The test equipment is schematically presented in Fig. 1. A fan pumps ambient air through a HEPA filter to the air inlet. The HEPA filter is of class H13 EN 1822 with a collection efficiency of 99.95 % at the maximum penetrating particle size, which ensures particle-free inlet air. The inlet air velocity was measured with a TSI® air velocity transducer model 8455. The air is assumed to be well mixed inside the box due to the complex volume of the pin-on-disc tribometer and the high air exchange rate [24]. The air inside the box transports the generated particles to the air outlet where the sampling point for the particle instruments is located. The temperature and humidity inside the box are measured but they are not controlled.

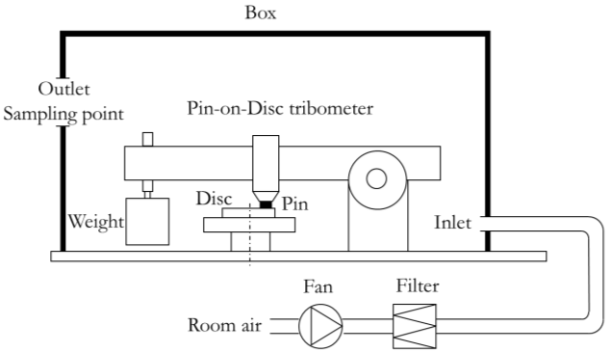

Fig. 1. Schematic image of the test equipment [23].

Three instruments were used to measure particle emissions. The first was a Dekati® Electrical Low-Pressure Impactor (ELPI+) which was used for real-time measurements of particle concentrations for particle diameters from 6 nm up to 10 μm. The second instrument was a TSI® Optical Particle Sizer (OPS) model 3330, which measures particle number concentrations in the size range 0.3 μm to 10 μm. The third instrument was a TSI® Condensation Particle Counter (CPC) model 3772 which counts particles with diameters from 10 nm up to >3 μm. The sampling frequency was 1 Hz for all three instruments. The ELPI instrument was used to measure mass concentration, while the OPS and CPC were used to measure number concentrations. With the concentration known, the particle number and mass rates (i.e., the number of particles or mass generated per sliding distance) can be calculated as [26]:

$$n = \frac{1}{s}\int_{t_1}^{t_2} c \cdot Q \cdot dt \tag{2}$$

where c is the measured number or mass concentration of the particles, Q is the air flow rate through the box, t_1 and t_2 are the start time and end time of the period studied, and s is the sliding distance between t_1 and t_2.

2.2 Test conditions

Wahlström et al. [23] used a reference car, a C-segment passenger car commonly used in Europe, to set the pin-on-disc tribometer sliding speed and nominal contact pressure. An image of the reference car left front disc brake can be seen Fig. 2. Table 1 shows the data of the reference car and brake system. The same reference car is used in the present work.

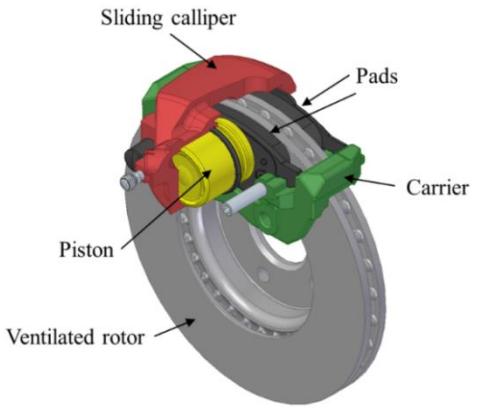

Fig. 2. Single piston sliding calliper disc brake.

Table 1. Data of the reference car and its front left disc brake.

Front wheel load	690 kg
Wheel radius	314 mm
Rotor outer radius	139 mm
Rotor inner radius	80 mm
Rotor effective radius	113 mm
Pad surface area	5080 mm^2
Cylinder diameter	57 mm

The tests were conducted with cylindrical pin specimens made of NAO pad material with diameter 10 mm and height of 8 mm. Disc specimens were made of AlSiC MMC rotor material of 54 mm diameter and 6 mm thickness. Both the NAO pad and AlSiC MMC rotor materials are commercial products and their chemical compositions are confidential. The only known information about the AlSiC MMC rotor is that it contains some 15 % SiC. The test specimens were directly cut-out from unused serial production parts and their surfaces were in as-received condition. The surface of the pin was scorched while the disc surface was grinded. The average R_a value of the unused disc is 1.8 μm, as measured by Taylor/Hobson Form TalySurf PGI 800. The densities of the pin and disc to calculate the specific wear rate are 2.6 g/m^3 and 3.0 g/m^3, respectively.

To be able to compare the results with Wahlström et al. [23], the same constant sliding speed (2 m/s) and nominal contact pressure (0.6 MPa) was tested in the present work. These setting corresponds to the mean contact pressures and mean disc temperatures as measured during a LACT test run with a brake inertia dynamometer and the reference disc brake. In the present work, the mid diameter of the wear track on the disc was set 38 mm. The rotational velocity of the disc was set to 984 rpm to get a sliding speed of 2 m/s. The nominal contact pressures to 0.5, 0.6, and 0.9 MPa. If scaled to the reference car, the sliding speed corresponds to a mean vehicle speed of about 20 km/h. The tests were run for 120 minutes, and the corresponding sliding distance was about 14.1 km in the middle of the wear track. Before each test commenced, the particle instruments were checked to ensure that there was negligible concentration inside the box. This check ensures that particles registered by the particle instruments during testing are generated from the sliding contact

and not the environment. After the tests ended, the particle instruments were also checked to determine whether the measured concentration was again negligible.

3. RESULTS

The measured coefficient of friction, particle number and mass concentrations are presented in Fig. 3 to Fig. 6, respectively. Photographs of the disc surfaces after testing can be seen in Fig. 7. The red circles mark where the holes for thermocouples were drilled in the discs. The average R_a value, as measured with TalySurf, of the black layer formed on the discs (see Fig. 7) is 0.16 µm and 1.25 µm in the rest of the wear track regardless of nominal contact pressure used.

Light optical microscope images of the disc surfaces after testing taken at different magnifications can be seen in Fig. 8 and Fig. 9. The light optical microscope images presented in Fig. 9 of the black layer which can be seen in the wear tracks of all tested discs (see Fig. 7).

The mean coefficient of friction (μ), mean particle number (c_{CPC}, c_{OPS}) and mass concentrations (c_{ELPI}), and mean inlet air speeds (v_{air}), between 6000 and 7000 seconds are shown in Table 2, along with disc temperature (T_{end}) measured at the end of the tests, the weight losses of the pins (Δm_{pin}) and discs (Δm_{disc}).

The specific wear rate of the pins (k_{pin}) and discs (k_{disc}), particle number rates (n_{OPS} and n_{FMPS}), and particle mass rate (n_{ELPI}) were calculated according to equations 1 and 2 (Table 3).

The test specimens run at a nominal contact pressure of 0.9 MPa were reused in a test at a nominal contact pressure of 0.5 MPa. This test is marked with an asterisk in Table 2 and 3.

Table 2. Mean coefficient of friction (μ), particle and mass number concentrations (c_{CPC}, c_{OPS}, c_{ELPI}), inlet air velocity (v_{air}), end disc temperature (T_{end}), pins (Δm_{pin}) and discs (Δm_{disc}) weight losses for NAO pins on AlSiC MMC rotors.

Test	0.5 MPa	0.6 MPa	0.9 MPa	0.5 MPa (*)
μ [-]	0.54	0.55	0.49	0.53
c_{CPC} [cm^{-3}]	447	104	186	104
c_{OPS} [cm^{-3}]	385	101	29	71
c_{ELPI} [mg m^{-3}]	0.54	0.26	0.16	0.21
v_{air} [m/s]	0.38	0.48	0.60	0.45
T_{end} [°C]	164	186	245	131
Δm_{pin} [mg]	57	64	88	20
Δm_{disc} [mg]	-3	-8	-10	-12

Table 3. Specific wear rate of pins (k_{pin}) and discs (k_{disc}), particle number rates (n_{CPC} and n_{OPS}) and mass rate (n_{ELPI}) for NAO pins on AlSiC MMC rotors.

Test	0.5 MPa	0.6 MPa	0.9 MPa	0.5 MPa (*)
k_{pin} [10^{-14} Pa^{-1}]	3.5	3.5	3.3	1.2
k_{disc} [10^{-15} Pa^{-1}]	-1.7	-4.1	-3.5	-6.7
n_{CPC} [#/m]	409000	121000	271000	114000
n_{OPS} [#/m]	352000	118000	43000	78000
n_{ELPI} [µg/m]	0.49	0.30	0.23	0.23

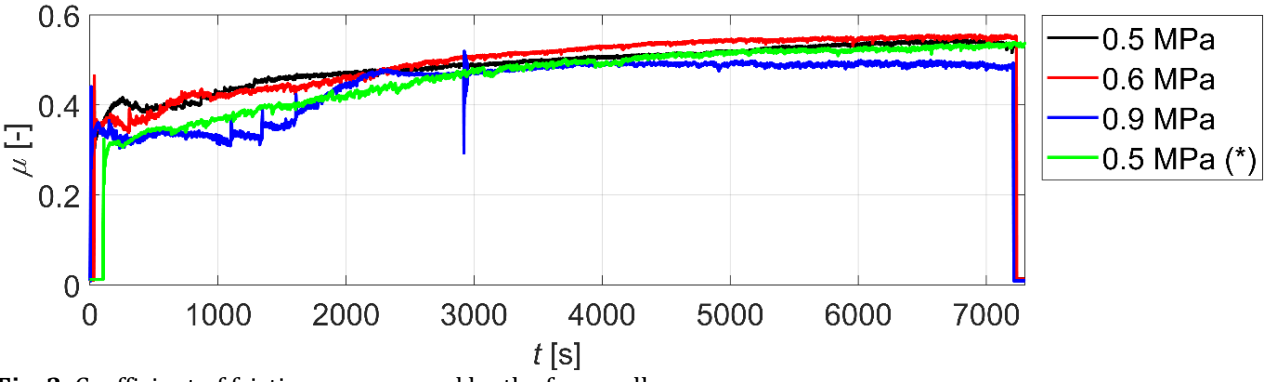

Fig. 3. Coefficient of friction as measured by the force cell.

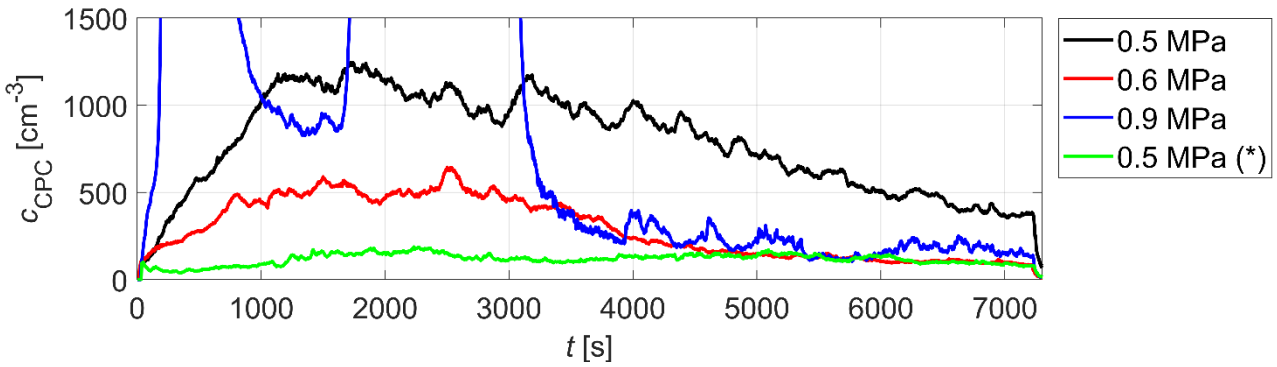

Fig. 4. Particle number concentration as measured by the CPC instrument.

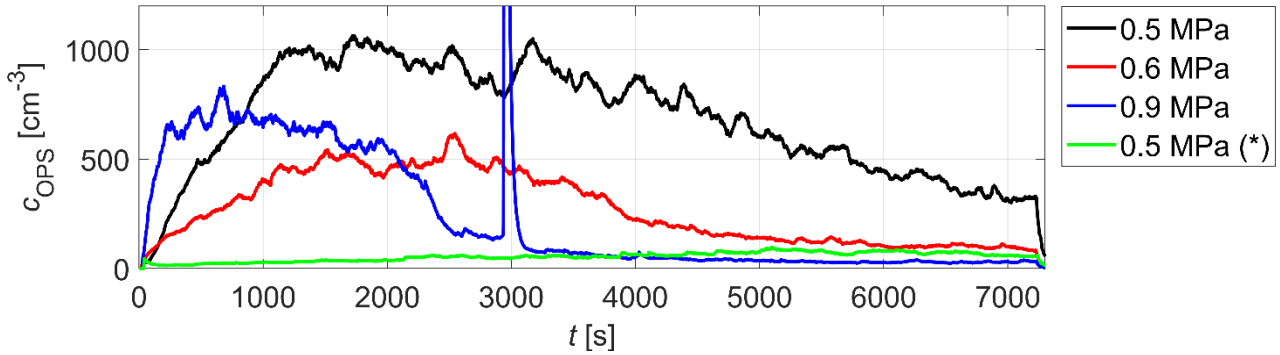

Fig. 5. Particle number concentration as measured by the OPS instrument.

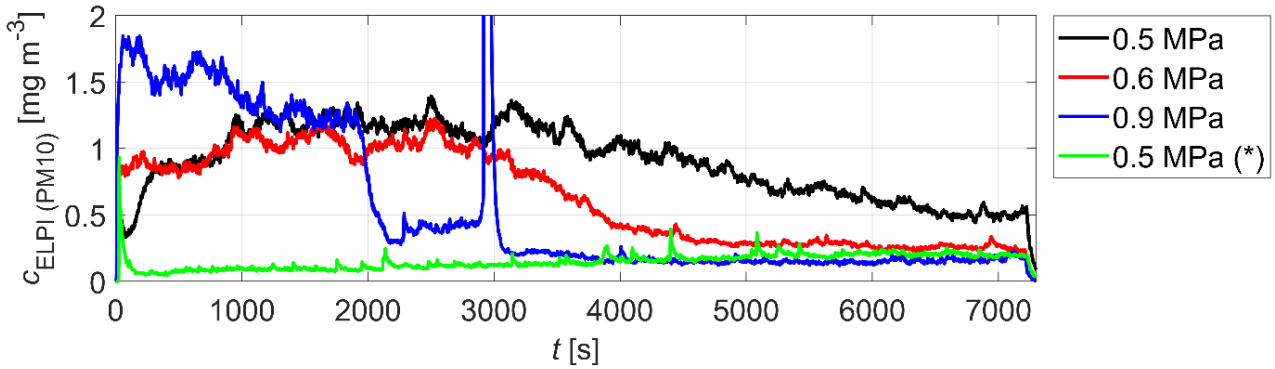

Fig. 6. Mass concentration (PM10) as measured by the ELPI+ instrument.

Fig. 7. Photographs of the wear tracks of the disc surfaces after testing at 0.5, 0.6, 0.9 MPa. The red circles mark where the holes for thermocouples were drilled.

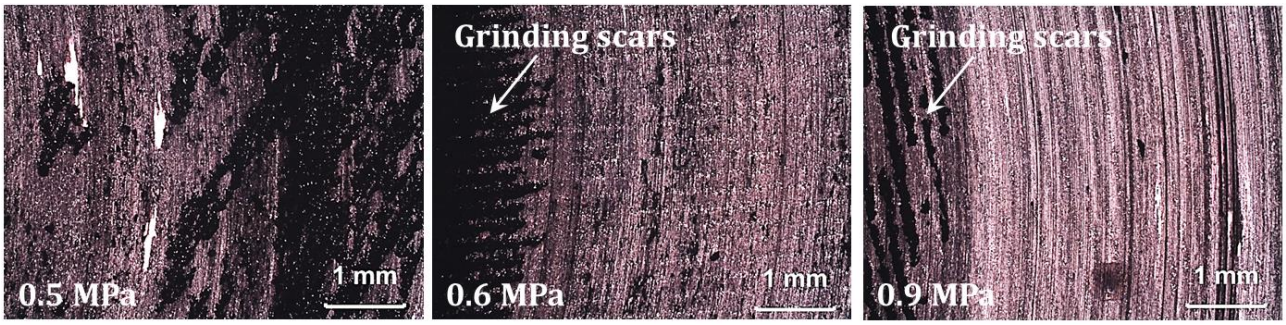

Fig. 8. Optical microscope images of the wear tracks on the disc surfaces after testing at nominal contact pressures of 0.5, 0.6, 0.9 MPa.

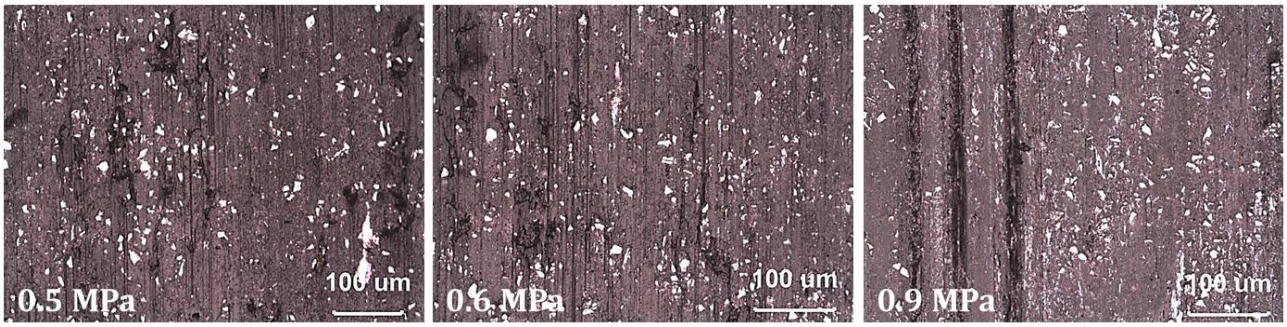

Fig. 9. Optical microscope images of the wear tracks on the disc surfaces after testing at nominal contact pressures of 0.5, 0.6, 0.9 MPa.

4. DISCUSSION

Wahlström et al. [23] tested eight disc brake material contact pairs in the same tribometer setup as used in this paper with a sliding speed of 2 m/s and a nominal contact pressure of 0.6 MPa. The results in terms of specific wear rate, particle number and mass rate for a conventional low-metallic pad (F1) and cast iron disc (D1) are shown in Table 4. These results are used as a baseline in the discussion.

Table 4. Mean coefficient of friction (μ), specific wear rate of the pin (k_{pin}) and disc (k_{disc}), particle number (n_{CPC} and n_{OPS}) and mass rates (n_{ELPI}) for a low-metallic pin sliding against a cast iron disc [23].

	F1/D1
μ [-]	0.50
k_{pin} [10^{-14} Pa^{-1}]	3.1
k_{disc} [10^{-15} Pa^{-1}]	3.6
n_{CPC} [#/m]	126000
n_{OPS} [#/m]	84000
n_{ELPI} [µg/m]	0.52

The mean coefficient of friction (Table 2) is relatively high in comparison to the conventional contact pair (Table 4) even though the pins were made from NAO pad material. NAO material is usually expected to have a lower coefficient of friction. Similar levels of coefficient of friction have been found in other pin-on-disc tests with AlSiC MMC brake contact pairs under similar contact pressures and sliding speeds [13–15]. This indicates that the friction performance of AlSiC MMC contact pairs is as good as conventional contact pairs at the tested conditions.

The tangential braking force should be about the same to be able to directly compare the specific wear and particle rates for different material combinations. With this in mind, the results of the 0.5 MPa tests (Table 2) are compared with the results of the 0.6 MPa test presented in Table 4. The specific wear rate of the pins that were not reused (first three columns of Table 3) is at the same level as the conventional pad material (Table 3). The test conducted with a pin that was reused after the 0.9 MPa test before it was tested at 0.5 MPa stands out in terms of specific wear rate (fourth column of Table 2). In this test, the specific wear rate of the pin is less than half that of the conventional pin (Table 4). The wear performance in terms of the specific wear rate of the disc tested is better than of a conventional disc.

The particle mass rate is lower than for the conventional contact pair. The test specimens show a decrease of about 50 % in particle mass rate. However, the particle number rates are higher for all tests except for the reused contact pair, which had approximately the conventional particle number rates. These results are promising since it seems to be possible to decrease the airborne emissions of finer particles by modifying the pad and/or the disc material in the future.

The contact pairs tested take up to 6000 seconds to reach a steady level in both friction (Fig. 3) and particle generation (Fig. 4 - Fig. 6), while the conventional contact pair only takes about 1500 seconds [23]. Also, the specific wear rates for the tested discs are negative, which means that material is added to the disc during testing. The added material can be seen as a black layer in the wear track of the discs shown in Fig. 7. It seems that a wear-resistant third body tribo-layer has been self-coated on the disc surfaces by the wear process. It can also be seen in Fig. 7 that the part of the wear track on the discs that has been self-coated increases with increased contact pressure and temperature. The black appearance of the wear track, which was also seen in [14] and [21], indicates that tribo-oxidation has a strong influence on the creation of the self-coating [4]. This third body tribo-layer is widely accepted as a protective coating and lubricant resulting in an improvement of the wear resistance of Al MMC brake discs [1,12,17]. Further, the protective tribo-layer forms more easily under higher load, suggesting a lower coefficient of friction under high load in comparison to that under low load [14,17]. In the current study, Al MMC brake discs also yielded a lower coefficient of friction at 0.9 MPa than at 0.5 and 0.6 MPa (Table 1). From the optical microscope image presented in Fig. 9 it seems that the tribo-layer created at different contact pressures are similar. This similarity was also seen in the surface roughness measurements which shows that the R_a of the tribo-layer is at a similar level. It should also be noted that the reused started and stopped at a lower emission level (Fig. 4 - Fig. 6).

The self-coating of the AlSiC MMC discs seems to be a slow process compared to the running-in of conventional disc brake contact pairs (Fig. 3-Fig. 6). It can be seen in Fig. 8 that the lowlands of the grinding scars of the discs seem to act as storage space for pin wear debris and that the highlands have already been in contact. The effect of the direction of the grinding scars can be glimpsed in Fig. 7. It seems easier to create the tribo-layer on the disc where the grinding scars are perpendicular to the sliding direction, especially for the disc run at 0.6 MPa. Blau et al. [5] characterized the wear particles produced from conventional cast iron and unconventional Al MMC disc brakes and found that the wear debris shows a large dependence on the surface features [5]. Copper fibres from the pin material can be seen on the disc surfaces (Fig. 7 and Fig. 8), which shows that material from the pins is added to the discs.

Note that the coating is more easily created at the part of the disc where holes were drilled for thermocouples (marked by red circles in Fig. 7). In these parts of the disc wear track, the temperature can be expected to be higher, since quite a lot of material was removed when drilling the holes. This indicates that the self-coating process strongly depends on the contact temperature, as reported in the literature. In future studies, the impact of initial disc surface pattern and different brake conditions should be studied.

5. CONCLUSION

The friction, wear and particle emission dependence of normal load for an AlSiC MMC brake disc/NAO brake pad system was studied using a pin-on-disc tribometer. The major conclusions that can be drawn are as follows:

- The friction performance from the tested AlSiC MMC brake contact pair is as good as a conventional brake contact pair.
- Under a similar braking condition, the specific wear rate of the tested brake pad material is at the same level as that of conventional brake pad material.
- AlSiC MMC brake discs yielded a negative specific wear rate and gained materials from the counterpart brake pad to form a protective third body tribo-layer. The protective tribo-layer is likely to be generated more easily under higher load.
- The surface grinding feature on the AlSiC MMC brake disc and the contact

temperature during braking seem to influence the formation of the tribo-layer.

- Reusing an AlSiC MMC disc run at a higher load to create the tribo-layer reduced the airborne emission in terms of mass by about 50%. The number of particles is about the same as with conventional brake pad material under a similar braking condition.
- Further studies at full scale (e.g., inertia brake dynamometer bench tests) are necessary to determine the validity of the findings in the current study.

Acknowledgement

The research leading to these results received funding from the European Union's Horizon 2020 research and innovation programme under grant agreement No. 636592 (LOWBRASYS project).

The authors also want to acknowledge the valuable help of Anders Eklund (Automotive Components Floby AB) who provided us with test specimens.

REFERENCES

[1] H. Nakanishi, K. Kakihara, A. Nakayama, T. Murayama, *Development of aluminum metal matrix composites (Al-MMC) brake rotor and pad*, Japanese Society of Automotive Engineers Review, vol. 23, iss. 3, pp. 365-370, 2002, doi: 10.1016/S0389-4304(02)00203-5

[2] A. Rehman, S. Das, G. Dixit, *Analysis of stir die cast Al–SiC composite brake drums based on coefficient of friction*, Tribology International, vol. 51, pp. 36-41, 2012, doi: 10.1016/j.triboint.2012.02.007

[3] S.V. Prasad, R. Asthana, *Aluminum metal-matrix composites for automotive applications: Tribological considerations*, Tribology Letters, vol. 17, iss. 3, pp. 445-453, 2004, doi: 10.1023/B:TRIL.0000044492.91991.f3

[4] I. Sallit, C. Richard, R. Adam, F. Robbe-Valloire, *Characterization methodology of a tribological couple: Metal matrix composite/brake pads*, Materials Characterization, vol. 40, iss. 3, pp. 169-188, 1998, doi: 10.1016/S1044-5803(98)00007-2

[5] P.J. Blau, H.M. Meyer, *Characteristics of wear particles produced during friction tests of conventional and unconventional disc brake materials*, Wear, vol. 255, iss. 7-12, pp. 1261-1269, 2003, doi: 10.1016/S0043-1648(03)00111-X

[6] P. Sadagopan, H.K. Natarajan, K.J. Praveen, *Study of silicon carbide-reinforced aluminum matrix composite brake rotor for motorcycle application*, The International Journal of Advanced Manufacturing Technology, vol. 94, iss. 1-4, pp. 1461-1475, 2018, doi: 10.1007/s00170-017-0969-7

[7] R.M. Harrison, A.M. Jones, J. Gietl, J. Yin, D.C. Green, *Estimation of the contributions of brake dust, tire wear, and resuspension to nonexhaust traffic particles derived from atmospheric measurements*, Environmental Science and Technology, vol. 46, no. 12, pp. 6523-6529, 2012, doi: 10.1021/es300894r

[8] T. Grigoratos, G. Martini, *Brake wear particle emissions: A review*, Environmental Science and Pollution Research, vol. 22, iss. 4, pp. 2491-2504, 2015, doi: 10.1007/s11356-014-3696-8

[9] J.T. Zelikoff, L.C. Chen, M.D. Cohen, K. Fang, T. Gordon, Y. Li, C. Nadziejko, R.B. Schlesinger, *Effects of inhaled ambient particulate matter on pulmonary antimicrobial immune defense*, Inhalation Toxicology, vol. 15, no. 2, pp. 131-150, 2003, doi: 10.1080/08958370304478

[10] J.M. Samet, D.M. DeMarini, H.V. Malling, *Do airborne particles induce heritable mutations?*, Science, vol. 304, iss. 5673, pp. 971-972, 2004, doi: 10.1126/science.1097441

[11] Y. Zhou, Y. Liu, Y. Song, J. Xie, X. Cui, B. Zhang, T. Shi, J. Yuan, W. Chen, *Short-term effects of outdoor air pollution on lung function among female non-smokers in China*, Scientific Reports, vol. 6, article 34947, 2016, doi: 10.1038/srep34947

[12] J. Wahlström, V. Matějka, Y. Lyu, A. Söderberg, *Contact Pressure and Sliding Velocity Maps of the Friction, Wear and Emission from a Low-Metallic/Cast-Iron Disc Brake Contact Pair*, Tribology in Industry, vol. 39, no. 4, pp. 460-470, 2017, doi: 10.24874/ti.2017.39.04.05

[13] S. Anoop, S. Natarajan, S.P. Kumaresh Babu, *Analysis of factors influencing dry sliding wear behaviour of Al/SiCp–brake pad tribosystem*, Materials and Design, vol. 30, iss. 9, pp. 3831-3838, 2009, doi: 10.1016/j.matdes.2009.03.034

[14] K. Laden, J.D. Guerin, M. Watremez, J.P. Bricout, *Frictional characteristics of Al-SiC composite brake discs*, Tribology Letters, vol. 8, iss. 4, pp. 237-247, 2000, doi: 10.1023/A:1019159923619

[15] A. Daoud, M.T. Abou El-khair, *Wear and friction behavior of sand cast brake rotor made of A359-20 vol% SiC particle composites sliding against*

automobile friction material, Tribology International, vol. 43, iss. 3, pp. 544-553, 2010, doi: 10.1016/j.triboint.2009.09.003

[16] M. Uthayakumar, S. Aravindan, K. Rajkumar, *Wear performance of Al–SiC–B4C hybrid composites under dry sliding conditions*, Materials and Design, vol. 47, pp. 456-464, 2013, doi: 10.1016/j.matdes.2012.11.059

[17] K.M. Shorowordi, A.S.M.A. Haseeb, J.P. Celis, *Velocity effects on the wear, friction and tribochemistry of aluminum MMC sliding against phenolic brake pad*, Wear, vol. 256, iss. 11-12, pp. 1176-1181, 2004, doi: 10.1016/j.wear.2003.08.002

[18] R.K. Uyyuru, M.K. Surappa, S. Brusethaug, *Tribological behavior of Al–Si–SiCp composites/automobile brake pad system under dry sliding conditions*, Tribology International, vol. 40, iss. 2, pp. 365-373, 2007, doi: 10.1016/j.triboint.2005.10.012

[19] S. Zhang, F. Wang, *Comparison of friction and wear performances of brake material dry sliding against two aluminum matrix composites reinforced with different SiC particles*, Journal of Materials Processing Technology, vol. 182, iss. 1-3, pp. 122-127, 2007, doi: 10.1016/j.jmatprotec.2006.07.018

[20] L. Pan, J. Han, Z. Yang, J. Wang, X. Li, Z. Li, W. Li, *Temperature Effects on the Friction and Wear Behaviors of SiCp/A356 Composite against Semimetallic Materials*, Advances in Materials Science and Engineering, vol. 2017, pp. 1-2, 2017, doi: 10.1155/2017/1824080

[21] K.M. Shorowordi, A.S.M.A. Haseeb, J.P. Celis, *Tribo-surface characteristics of Al–B4C and Al–SiC composites worn under different contact pressures*, Wear, vol. 261, iss. 5-6, pp. 634-641, 2006, doi: 10.1016/j.wear.2006.01.023

[22] R.C. Shivamurthy, M.K. Surappa, *Tribological characteristics of A356 Al alloy–SiCP composite discs*, Wear, vol. 271, iss. 9-10, pp. 1946-1950, 2011, doi: 10.1016/j.wear.2011.01.075

[23] J. Wahlström, Y. Lyu, V. Matjeka, A. Söderberg, *A pin-on-disc tribometer study of disc brake contact pairs with respect to wear and airborne particle emissions*, Wear, vol. 384-385, pp. 124-130, 2017, doi: 10.1016/j.wear.2017.05.011

[24] J. Archard, W. Hirst, *The wear of metals under unlubricated conditions*, Proceedings of The Royal Society A, vol. 236, iss. 1206, pp. 397-410, 1956, doi: 10.1098/rspa.1956.0144

[25] G. Riva, J. Wahlström, M. Alemani, U. Olofsson, *A CFD study of a pin-on-disc tribometer setup focusing on airborne particle sampling efficiency*, in 6th European Conference on Tribology, 7-9 June, 2017, Ecotrib 2017, Ljubljana, Slovenia, 2017.

[26] J. Wahlström, *A comparison of measured and simulated friction, wear, and particle emission of disc brakes*, Tribology International, vol. 92, pp. 503-511, 2015, doi: 10.1016/j.triboint.2015.07.036